Electronic Supplementary Material (ESI) for Journal of Materials Chemistry C.

Supporting Information

Engineering dual charge transfer materials modified $Zn_xCd_{1-x}S$ towards highly effective photocatalytic pure water splitting

Meiling Xu,[ab] Chaomin Gao,*[b] Shan Yao,[b] Shubo Sun,[a] Lina Zhang,[a] Kui Li,[c] Xin Cheng*[a]

[a]Shandong Provincial Key Laboratory of Preparation and Measurement of Building Materials, University of Jinan, Jinan, 250022, PR China. E-mail: chengxin@ujn.edu.cn.
[b]School of Chemistry and Chemical Engineering, University of Jinan, Jinan, 250022, PR China. E-mail: chm_gaocm@163.com.
[c]School of Materials Science and Engineering, University of Jinan, Jinan 250022, China.

1. Experimental section

1.1 Materials Characterization

Powder X-ray diffraction (XRD, D8 Advance, Bruker) patterns were taken by using a Rigaku-miniflex 6 powder X-ray diffractometer equipped with Cu-Ka (λ=0.15406 nm) radiation with a scan rate of 10° min^{-1} at 2θ ranging from 5° to 80°. The morphologies of the resultant samples were observed by a field emission scanning electron microscope (SEM) (JSM-6700F, JEOL) and a transmission electron microscopy (TEM) (JEM-2100, JEOL). The elementary composition of samples was analyzed with the energy dispersive spectrometer (EDS) (JSM-6700F, JEOL) and elemental mapping. The X-ray photoelectron spectroscopy (XPS) spectra were analyzed by a Thermo Fisher Scientific corporation Escalab 250Xi instrument. The Brunauer-Emmett-Teller (BET) specific surface areas were recorded on an automatic BET analyzer (Autosorb-iQ-TPX, Auantachrome), and the products were degassed at 90 °C for 6 h before the N_2 adsorption measurements. Ultraviolet-visible (UV-vis) diffuse reflectance spectra (DRS) were obtained using a UV-vis spectrophotometer (UH4150, HITACHI). Steady photoluminescence (PL) emission spectra were tested by a luminescence spectrophotometer (QM-400, PTI) with 350 nm excitation wavelength.

1.2 Photocatalytic Experiments

The photocatalytic water splitting experiments were performed in a 100 mL Pyrex flask at ambient temperature and atmospheric pressure. A 300 W xenon arc lamp equipped with a 420-800 nm UV-cutoff filter was positioned 13 cm away from the reaction solution, acting as the visible light source to trigger the photocatalytic reaction. The focused intensity on the flask was about 100 $mW \cdot cm^{-2}$, measuring with a FZ-A visible-light radiometer (CEAULight, China). In a typical photocatalytic H_2-production experiment, 10 mg of the prepared photocatalyst was suspended in 50 mL pure water. Before irradiation, the system was vacuumed for 30 min via the vacuum pump to completely remove the dissolved oxygen and ensure the reactor was in an anaerobic condition. A continuous magnetic stirrer was applied at the bottom of the reactor to keep the photocatalyst particles in suspension during the experiments. H_2 content was analyzed by gas chromatography (GC-7900, CEAULight, China) with a TCD detector. H_2O_2 concentration was measured by a DPD-POD method. Briefly, 1 mL of sample aliquots was added to a mixture of 3 mL of phosphate buffer (0.5 M, pH = 6.0), 5.9 mL of water, 0.05 mL of DPD (10 mg/mL) and 0.05 mL of POD (1 mg/mL).

After 50 s, the H_2O_2 concentration was measured at 551 nm on a UV-vis spectrophotometer.

1.4 Photoelectrochemical Measurements

Photoelectrochemical characterizations were proceeded in Na_2SO_4 (0.5 M) solution with a standard three-electrode system on the electrochemical station (Bio-Logic SP-150). The carbon cloth coated with catalyst, Pt net and saturated Ag/AgCl were served as working electrode, counter electrode and reference electrode, respectively. Typically, a slurry of 4 mg of sample and 1 ml of ethanol were used to make the working electrode. The EIS was recorded from 0.01 Hz to 100 kHz with a sinusoidal ac perturbation of 10 mV. The impedance potential model was employed to collect the Mott-Schottky plots with the frequency of 500,1000 and 2000 Hz. I-t curves were recorded using 300 W Xe lamp with a 420 nm cutoff filter. The linear sweep voltammetry (LSV) for the HER and OER of the samples was tested by a Bio-Logic SP-150 type electrochemical station with the three-electrode system in 1 M KOH aqueous solution.

2. Supporting Figures

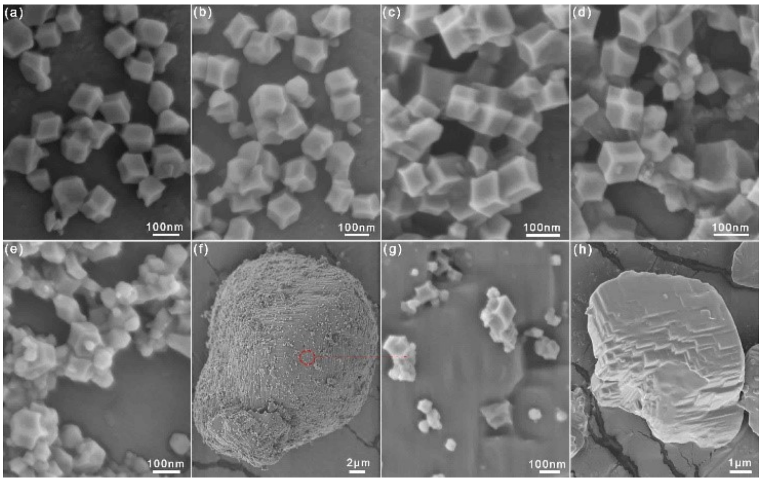

Fig. S1 SEM images of $Zn_{1-x}Cd_x$-ZIF (a) x=0, (b) x=0.1, (c) x=0.3, (d) x=0.5, (e) x=0.7, (f-g) x=0.9, (h) x=1.

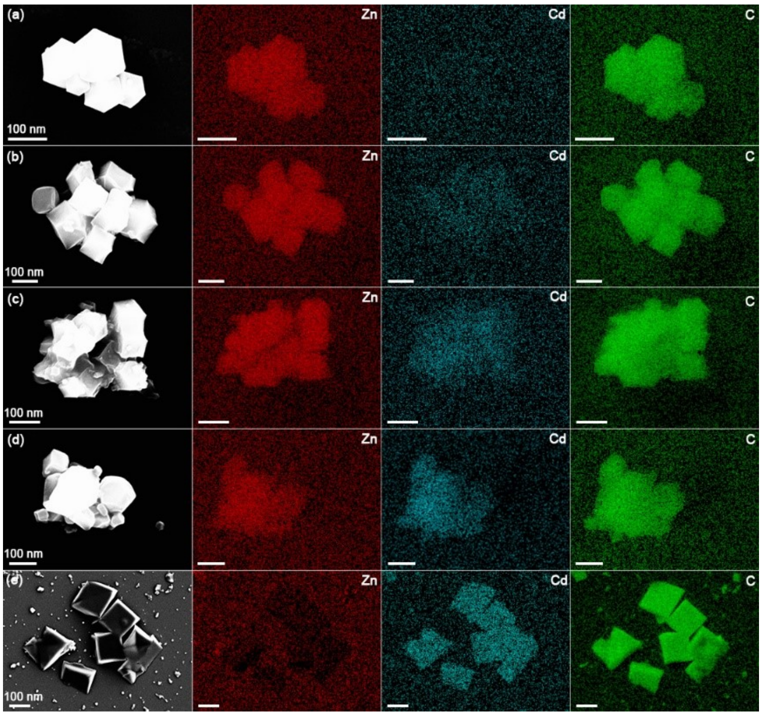

Fig. S2 EDS mapping images of $Zn_{1-x}Cd_x$-ZIF (a) x=0.1, (b) x=0.3, (c) x=0.5, (d) x=0.7, (e) x=0.9.

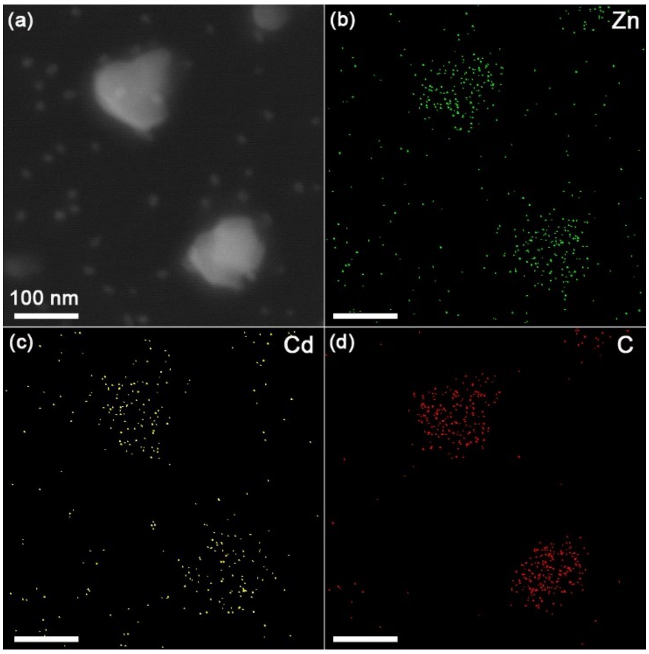

Fig. S3 EDX mapping images of $Zn_{0.5}Cd_{0.5}$-ZIF.

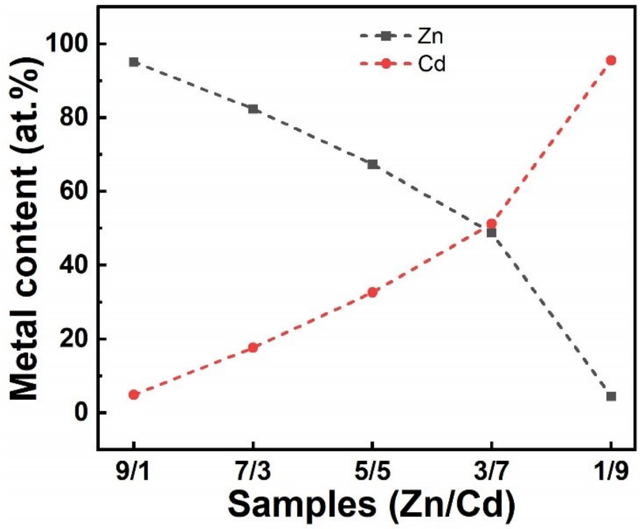

Fig. S4 Composition in the $Zn_{1-x}Cd_x$-ZIF with different molar ratios of Zn/Cd.

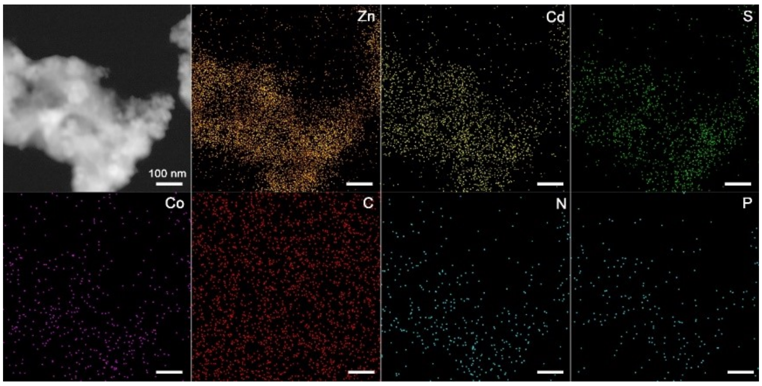

Fig. S5 X-ray elemental mappings of Co@NC/$Zn_{0.5}Cd_{0.5}S$/Co-Pi.

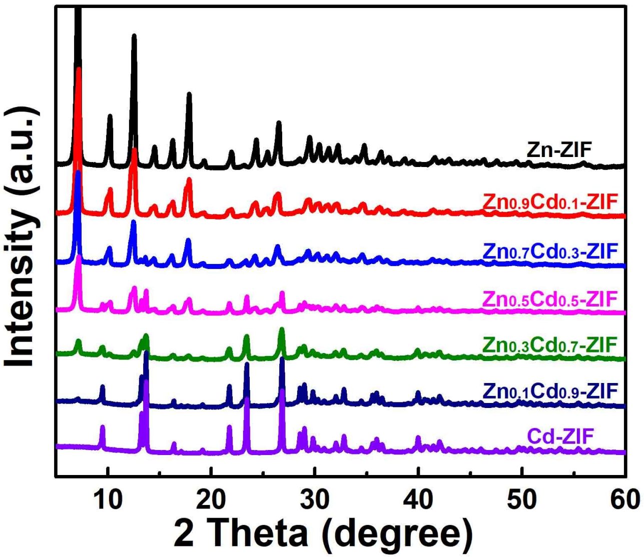

Fig. S6 XRD spectra of $Zn_{1-x}Cd_x$-ZIF samples.

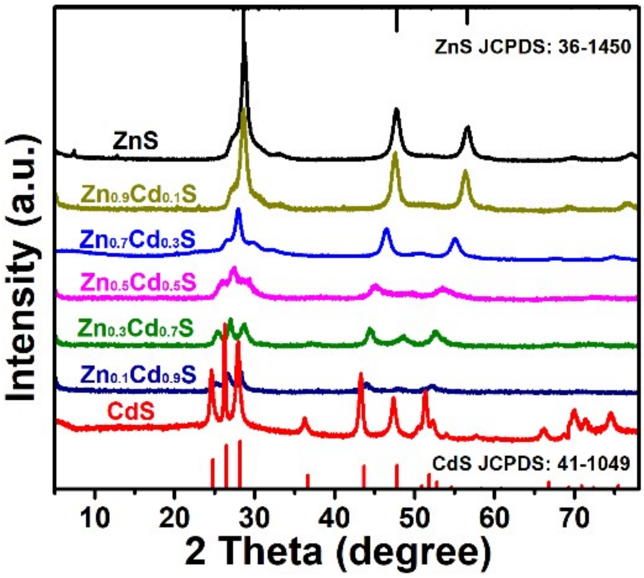

Fig. S7 XRD spectra of $Zn_{1-x}Cd_xS$ samples.

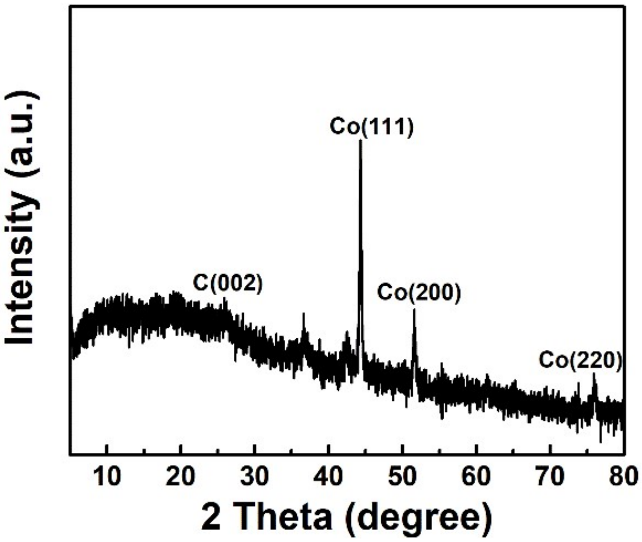

Fig. S8 XRD spectra of Co@NC samples.

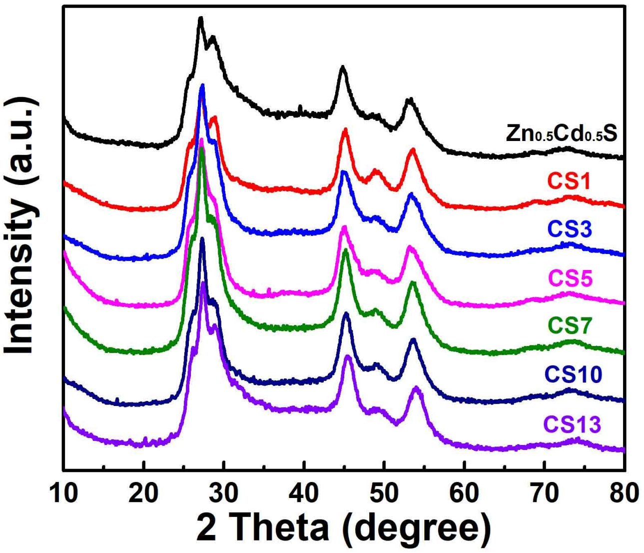

Fig. S9 XRD spectra of $Zn_{0.5}Cd_{0.5}S$ with different amount of Co@NC.

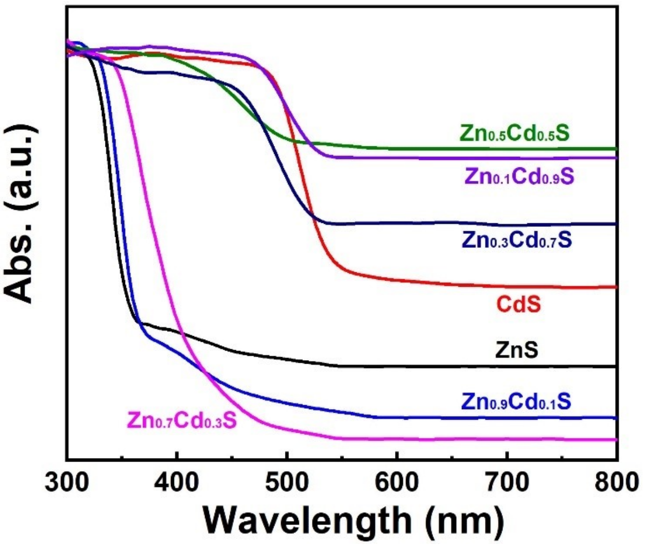

Fig. S10 UV-vis diffuse reflection spectra of $Zn_{1-x}Cd_xS$ samples.

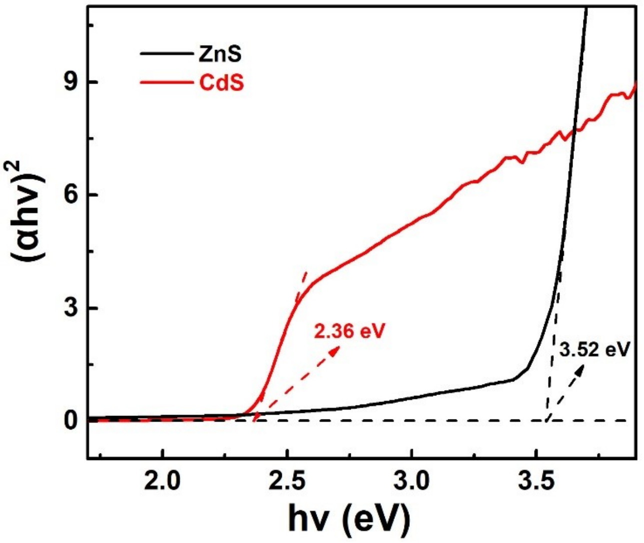

Fig. S11 The plot of transformed Kubelka-Munk function vs. the energy of ZnS and CdS.

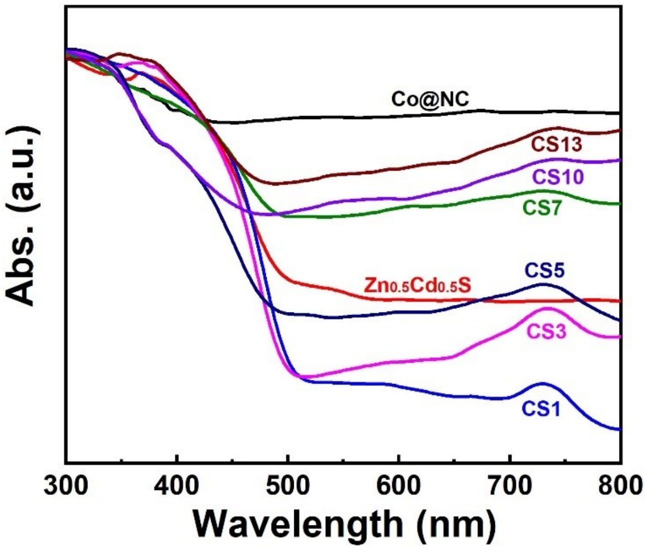

Fig. S12 UV-vis diffuse reflection spectra of $Zn_{0.5}Cd_{0.5}S$ with different amount of Co@NC.

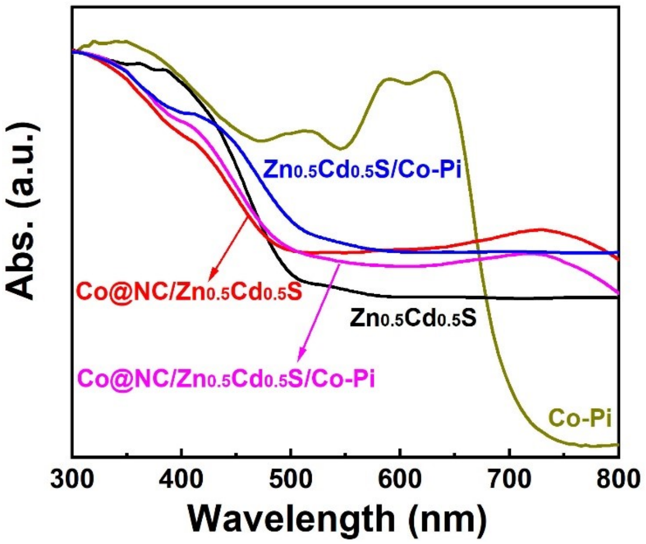

Fig. S13 UV-vis diffuse reflectance spectra of Co-Pi, $Zn_{0.5}Cd_{0.5}S$, Co@NC/$Zn_{0.5}Cd_{0.5}S$, $Zn_{0.5}Cd_{0.5}S$/Co-Pi and Co@NC/$Zn_{0.5}Cd_{0.5}S$/Co-Pi samples.

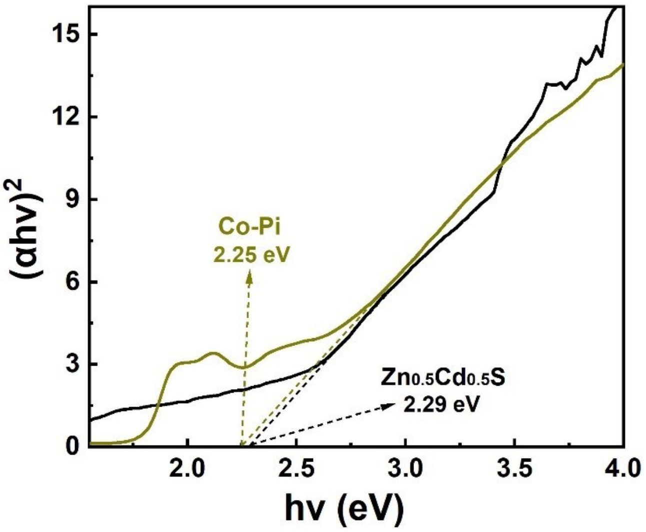

Fig. S14 The plot of transformed Kubelka-Munk function vs. the energy of $Zn_{0.5}Cd_{0.5}S$ and Co-Pi.

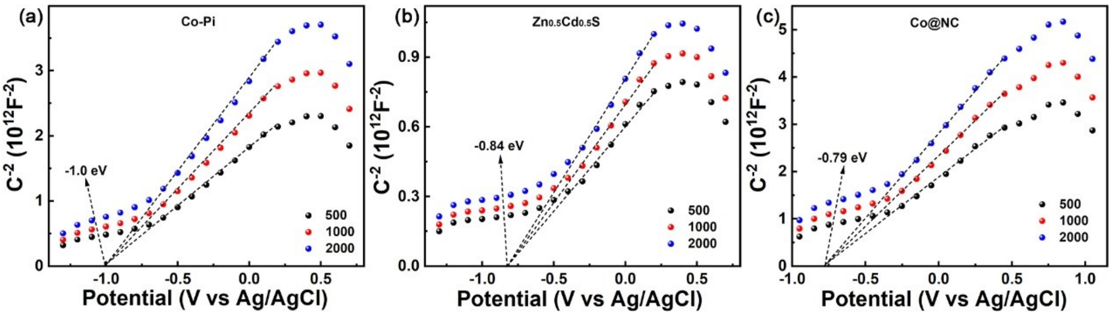

Fig. S15 Mott-Schottky plots of Co-Pi, $Zn_{0.5}Cd_{0.5}S$ and Co@NC.

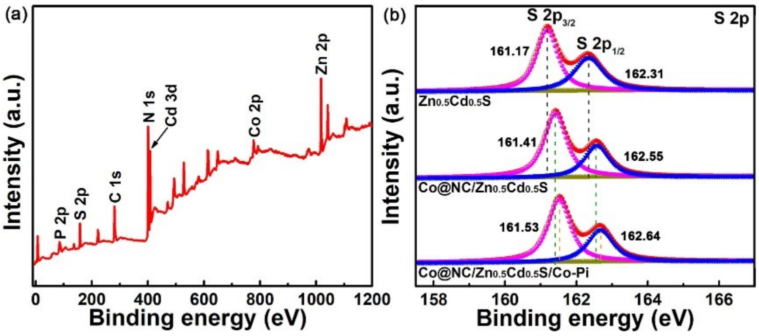

Fig. S16 X-ray photoelectron spectra (XPS) of (a) survey spectra for Co@NC/$Zn_{0.5}Cd_{0.5}S$/Co-Pi, (b) S 2p for $Zn_{0.5}Cd_{0.5}S$, Co@NC/$Zn_{0.5}Cd_{0.5}S$ and Co@NC/$Zn_{0.5}Cd_{0.5}S$/Co-Pi.

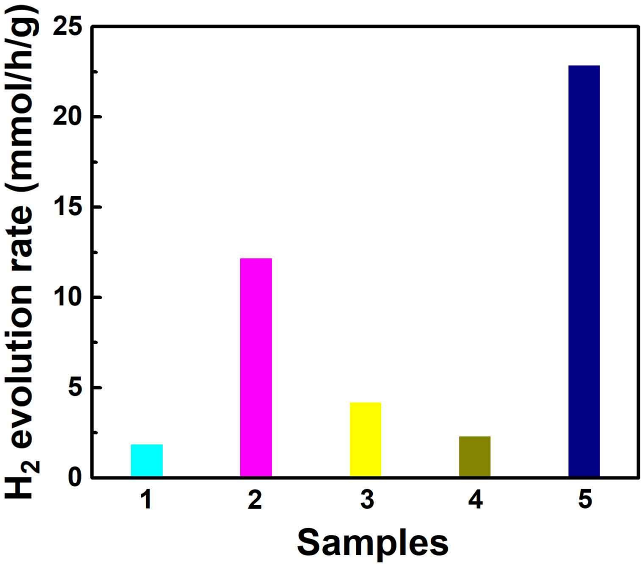

Fig. S17 Comparative results of the photocatalytic hydrogen production activity of $Zn_{0.5}Cd_{0.5}S$(1), Co@NC/$Zn_{0.5}Cd_{0.5}S$(2), Pt/$Zn_{0.5}Cd_{0.5}S$ (3), $Zn_{0.5}Cd_{0.5}S$/Co-Pi(4), Co@NC/$Zn_{0.5}Cd_{0.5}S$/Co-Pi(5) samples. Conditions: photocatalyst (10 mg); 0.35 M Na_2S and 0.25 M Na_2SO_3 solution (50 mL); light source, 300-W Xe lamp with a cut-off filter of 420 nm.

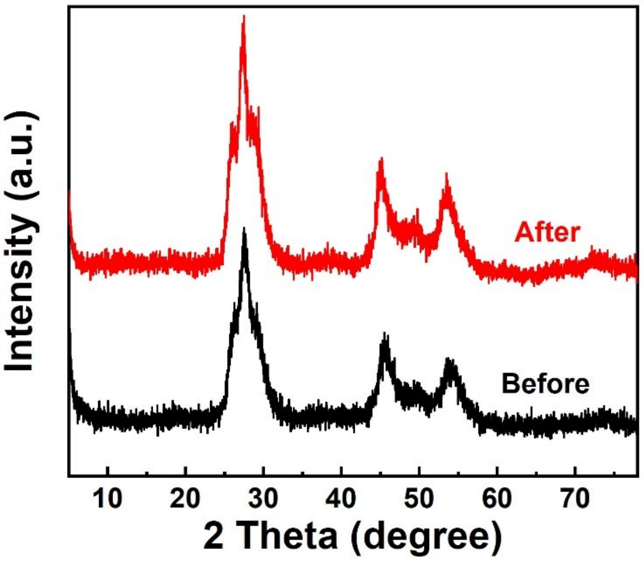

Fig. S18 The XRD patterns of Co@NC/$Zn_{0.5}Cd_{0.5}S$/Co-Pi before and after the photocatalytic reaction in pure water under visible light.

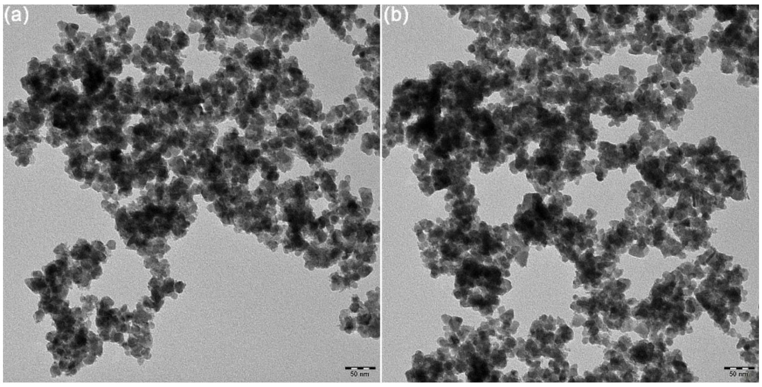

Fig. S19 TEM image of Co@NC/$Zn_{0.5}Cd_{0.5}S$/Co-Pi before and after the photocatalytic reaction in pure water under visible light.

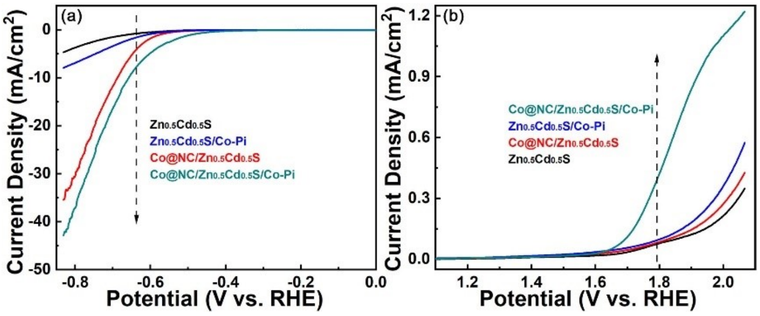

Fig. S20 The electrocatalytic HER and OER of $Zn_{0.5}Cd_{0.5}S$, Co@NC/$Zn_{0.5}Cd_{0.5}S$, $Zn_{0.5}Cd_{0.5}S$/Co-Pi and Co@NC/$Zn_{0.5}Cd_{0.5}S$/Co-Pi samples.

3. Supporting Tables

Table S1 Physicochemical properties of $Zn_{0.5}Cd_{0.5}S$, Co@NC/$Zn_{0.5}Cd_{0.5}S$, $Zn_{0.5}Cd_{0.5}S$/Co-Pi and Co@NC/$Zn_{0.5}Cd_{0.5}S$/Co-Pi samples.

Sample	S_{BET}(m^2/g)	Average pore size (nm)	Pore volume (cm^3/g)
$Zn_{0.5}Cd_{0.5}S$	69	24.62	0.41
Co@NC/$Zn_{0.5}Cd_{0.5}S$	115	14.23	0.58
$Zn_{0.5}Cd_{0.5}S$/Co-Pi	96	16.47	0.49
Co@NC/$Zn_{0.5}Cd_{0.5}S$/Co-Pi	128	13.69	0.62

Table S2 Comparison of the photocatalytic H_2 generation activities in pure water and apparent quantum efficiencie of sulfide-based composites.

Photocatalyst	Activity (μmol/h/g)	AQE/AQY (%)	Refs
Co@NC/$Zn_{0.5}Cd_{0.5}S$/Co-Pi	613.8	2.73@420 nm	This work
CdS/Ni_2P/gC_3N_4	15.6	0.18@420 nm	1
MCo_2O_4/ZnCdS	551	--	2
CDs-CdS	51	--	3
MoS_2/CdS	145	1.04@420 nm	4
$BiVO_4$/Au/CdS	281	--	5
MoS_2-CdS/WO_3-MnO_2	1.27	--	6
Pt/CdS@Al_2O_3	62.1	0.11@430 nm	7
Ag-$ZnIn_2S_4$	56.6	0.57@420 nm	8
$Bi_2O_{2.33}$/Bi_2S_3	196	--	9
Pt-TiO_2/CdS	3.074	0.17@430 nm	10
MnS/CoS_2/CDs	4.21	--	11
CdS-P	231	--	12
Ni_4P_2-CQDs@CdS	145	--	13
RuO_2/CdS/MoS_2	52	0.23@425 nm	14
ZnTHPP/CdS	68.9	--	15
CdS/WO_3/$CdWO_4$	6.08	--	16
$Cd_{0.5}Zn_{0.5}S$	248	--	17
$Cd_{0.5}Zn_{0.5}S$-$BiVO_4$	45.6	--	18
TiO_2-$ZnIn_2S_4$	214.9	--	19
CdS@Cr_2O_3	63.3	--	20

Table S3 Calculated apparent quantum efficiency (AQE) of Co@NC/$Zn_{0.5}Cd_{0.5}S$/Co-Pi at different wavelengths.

Sample	Wavelength (nm)	H_2 Evolved (μmol)	Light Intensity (mW)	AQE (%)
Co@NC/$Zn_{0.5}Cd_{0.5}S$/Co-Pi	420	2.26	13.1	2.73
	475	1.13	18.4	0.97
	550	0.54	20.3	0.42
	650	0.38	16.5	0.36

λ=420 nm

$$N=\frac{E\lambda}{hc}=\frac{13.1\times 10^{-3}\times 3600\times 420\times 10^{-9}}{6.626\times 10^{-34}\times 3\times 10^{8}}=9.96\times 10^{19}$$

$$AQE=\frac{the\ number\ of\ reacted\ electrons}{the\ number\ of\ incident\ photons}\times 100\%$$

$$=\frac{2\times the\ number\ of\ evolved\ H_2\ molecules}{N}\times 100\%$$

$$=\frac{2\times 6.02\times 10^{23}\times 2.26\times 10^{-6}}{9.96\times 10^{19}}=2.73\%$$

λ=475 nm

$$N=\frac{E\lambda}{hc}=\frac{18.4\times 10^{-3}\times 3600\times 475\times 10^{-9}}{6.626\times 10^{-34}\times 3\times 10^{8}}=1.58\times 10^{20}$$

$$AQE=\frac{the\ number\ of\ reacted\ electrons}{the\ number\ of\ incident\ photons}\times 100\%$$

$$=\frac{2\times the\ number\ of\ evolved\ H_2\ molecules}{N}\times 100\%$$

$$=\frac{2\times 6.02\times 10^{23}\times 1.13\times 10^{-6}}{1.58\times 10^{20}}=0.97\%$$

λ=550 nm

$$N=\frac{E\lambda}{hc}=\frac{20.3\times 10^{-3}\times 3600\times 550\times 10^{-9}}{6.626\times 10^{-34}\times 3\times 10^{8}}=2.02\times 10^{20}$$

$$AQE=\frac{the\ number\ of\ reacted\ electrons}{the\ number\ of\ incident\ photons}\times 100\%$$

$$=\frac{2\times the\ number\ of\ evolved\ H_2\ molecules}{N}\times 100\%$$

$$= \frac{2 \times 6.02 \times 10^{23} \times 0.54 \times 10^{-6}}{2.02 \times 10^{20}} = 0.42\%$$

λ=650 nm

$$N = \frac{E\lambda}{hc} = \frac{16.5 \times 10^{-3} \times 3600 \times 650 \times 10^{-9}}{6.626 \times 10^{-34} \times 3 \times 10^{8}} = 1.94 \times 10^{20}$$

$$AQE = \frac{the\ number\ of\ reacted\ electrons}{the\ number\ of\ incident\ photons} \times 100\%$$

$$= \frac{2 \times the\ number\ of\ evolved\ H_2\ molecules}{N} \times 100\%$$

$$= \frac{2 \times 6.02 \times 10^{23} \times 0.38 \times 10^{-6}}{1.94 \times 10^{20}} = 0.36\%$$

Table S4 Fluorescence emission lifetime and relevant percentage data fitted by a three-exponential function.

Sample	τ_1 (ns)	A_1 (%)	τ_2 (ns)	A_2 (%)	τ_3 (ns)	A_3 (%)	Average lifetime (ns)
$Zn_{0.5}Cd_{0.5}S$	6.93	0.12	1.92	0.38	0.69	0.55	1.04
Co@NC/$Zn_{0.5}Cd_{0.5}S$	0.79	0.49	0.94	0.35	3.47	0.04	3.14
$Zn_{0.5}Cd_{0.5}S$/Co-Pi	2.15	0.14	0.78	0.77	10.96	0.02	1.28
Co@NC/$Zn_{0.5}Cd_{0.5}S$/Co-Pi	2.43	0.06	0.81	0.51	0.24	0.55	3.83

Table S5 Resistance value (Rs and Rc) of $Zn_{0.5}Cd_{0.5}S$, Co@NC/$Zn_{0.5}Cd_{0.5}S$, $Zn_{0.5}Cd_{0.5}S$/Co-Pi and Co@NC/$Zn_{0.5}Cd_{0.5}S$/Co-Pi samples.

Sample	Rs (Ω)	Rc (Ω)
$Zn_{0.5}Cd_{0.5}S$	5.13	9.52
Co@NC/$Zn_{0.5}Cd_{0.5}S$	2.78	5.02
$Zn_{0.5}Cd_{0.5}S$/Co-Pi	3.65	6.67
Co@NC/$Zn_{0.5}Cd_{0.5}S$/Co-Pi	2.01	3.76

Supporting References

1 H. He, J. Cao, M. Guo, H. Lin, J. Zhang, Y. Chen and S. Chen, *Appl. Catal. B,* 2019, **249**, 246-256.

2 M. Chen, X. Huang, C. Chen, W. Hou and Y. Xu, *Appl. Catal. B,* 2021, **298**, 120469.

3 C. Zhu, C. Liu, Y. Zhou, Y. Fu, S. Guo, H. Li, S. Zhao, H. Huang, Y. Liu and Z. Kang, *Appl. Catal. B,* 2017, **216**, 114-121.

4 Y.-J. Yuan, D. Chen, S. Yang, L.-X. Yang, J.-J. Wang, D. Cao, W. Tu, Z.-T. Yu and Z.-G. Zou, *J. Mater. Chem. A,* 2017, **5**, 21205-21213.

5 X. Xu, Z. Wang, W. Qiao, F. Luo, J. Hu, D. Wang and Y. Zhou, *Int. J. Hydrogen Energy,* 2021, **46**, 8531-8538.

6 D. Wei, Y. Ding and Z. Li, *Int. J. Hydrogen Energy,* 2020, **45**, 17320-17328.

7 X. Ning, W. Zhen, Y. Wu and G. Lu, *Appl. Catal. B,* 2018, **226**, 373-383.

8 R. Pan, M. Hu, J. Liu, D. Li, X. Wan, H. Wang, Y. Li, X. Zhang, X. Wang, J. Jiang and J. Zhang, *Nano Lett,* 2021, **21**, 6228-6236.

9 Y. Ma, X. Jiang, R. Sun, J. Yang, X. Jiang, Z. Liu, M. Xie, E. Xie and W. Han, *Chem. Eng. J.,* 2020, **382**, 123020.

10 X. Ning, J. Li, B. Yang, W. Zhen, Z. Li, B. Tian and G. Lu, *Appl. Catal. B,* 2017, **212**, 129-139.

11 Y. Fu, C. Zhu, C. Liu, M. Zhang, H. Wang, W. Shi, H. Huang, Y. Liu and Z. Kang, *Appl. Catal. B,* 2018, **226**, 295-302.

12 R. Shi, H. F. Ye, F. Liang, Z. Wang, K. Li, Y. Weng, Z. Lin, W. F. Fu, C. M. Che and Y. Chen, *Adv. Mater,* 2018, **30**, 1705941.

13 Y. Dong, Q. Han, Q. Hu, C. Xu, C. Dong, Y. Peng, Y. Ding and Y. Lan, *Appl. Catal. B,* 2021, **293**, 120214.

14 B. Qiu, L. Cai, N. Zhang, X. Tao and Y. Chai, *Adv. Sci.,* 2020, **7**, 1903568.

15 X. Ning, Y. Wu, X. Ma, Z. Zhang, R. Gao, J. Chen, D. Shan and X. Lu, *Adv. Funct. Mater.,* 2019, **29**, 1902992.

16 H. Nagakawa, T. Ochiai, S. Konuma and M. Nagata, *ACS Appl. Energy Mater.,* 2018, **1**, 6730-6735.

17 W. Xue, X. Bai, J. Tian, X. Ma, X. Hu, J. Fan and E. Liu, *Chem. Eng. J.,* 2022, **428**, 132608.

18 C. Zeng, Y. Hu, T. Zhang, F. Dong, Y. Zhang and H. Huang, *J. Mater. Chem. A,* 2018, **6**, 16932-16942.

19 G. Zuo, Y. Wang, W. L. Teo, Q. Xian and Y. Zhao, *Appl. Catal. B,* 2021, **291**, 120126.

20 B. Tian, W. Gao, X. Zhang, Y. Wu and G. Lu, *Appl. Catal. B,* 2018, **221**, 618-625.